

Analytical Methods

Accepted Manuscript



This is an *Accepted Manuscript*, which has been through the Royal Society of Chemistry peer review process and has been accepted for publication.

Accepted Manuscripts are published online shortly after acceptance, before technical editing, formatting and proof reading. Using this free service, authors can make their results available to the community, in citable form, before we publish the edited article. We will replace this *Accepted Manuscript* with the edited and formatted *Advance Article* as soon as it is available.

You can find more information about *Accepted Manuscripts* in the [Information for Authors](#).

Please note that technical editing may introduce minor changes to the text and/or graphics, which may alter content. The journal's standard [Terms & Conditions](#) and the [Ethical guidelines](#) still apply. In no event shall the Royal Society of Chemistry be held responsible for any errors or omissions in this *Accepted Manuscript* or any consequences arising from the use of any information it contains.

1
2
3
4
5
6
7
8
9
10
11
12
13
14
15
16
17
18
19
20
21
22
23
24
25
26
27
28
29
30
31
32
33
34
35
36
37
38
39
40
41
42
43
44
45
46
47
48
49
50
51
52
53
54
55
56
57
58
59
60

Assessment of organosilane-functionalized nano-carbon black for interference-free on-line Pb(II) ions enrichment in water, herb medicines and environmental samples

Daniel Morais Nanicuacia¹, Mariana Gava Segatelli¹, Marcela Zanetti Corazza^{1,2}, César Ricardo Teixeira Tarley^{1,3*}

¹ Universidade Estadual de Londrina (UEL), Departamento de Química, Centro de Ciências Exatas, Rodovia Celso Garcia Cid, PR 445, Km 380, Londrina, PR, 86050-482, Brazil.

² Faculdade de Ciências Exatas e Tecnologia, FACET, Universidade Federal da Grande Dourados, Dourados, MS, 79804-970, Brazil.

³ Instituto Nacional de Ciência e Tecnologia (INCT) de Bioanalítica, Universidade Estadual de Campinas (UNICAMP), Instituto de Química, Departamento de Química Analítica, Cidade Universitária Zeferino Vaz, s/n, Campinas, SP, 13083-970, Brazil.

* Corresponding author. Tel +55 43 3371 4366; fax +55 43 3371 4286
E-mail address: ctarleyquim@yahoo.com.br (C. R. T. Tarley)

ABSTRACT

In the present work, commercial nano-carbon black particles (CB) were functionalized with 3-mercaptopropyltrimethoxysilane (3-MPTMS) through silanization reaction to improve their adsorption capacity towards the Pb(II) ions and hence extend their application as an alternative and low-cost nanocarbonaceous material in the field of separation science. The material was characterized by FT-IR, scanning electron microscopy (SEM), energy dispersive spectroscopy (EDS), Raman spectroscopy, as well as by thermogravimetric analysis and textural data. After the characterization of material (3-MPTMS/CB) a FIA-FAAS preconcentration method for Pb(II) ions was developed, which in turn was performed by loading 20.0 mL of a 200 $\mu\text{g L}^{-1}$ Pb(II) solution at pH 4.76 (buffered with 0.0358 mol L^{-1} acetate buffer) through 100 mg of 3-MPTMS/CB packed into a mini-column at a flow rate of 4.0 mL min^{-1} . The optimized condition of the proposed method has been achieved through a 2^{5-1} fractional factorial and Doehlert matrix design. The improvements on the adsorption capacity of CB towards the Pb(II) after chemical modification with 3-MPTMS was noticed by comparing the sensitivity of analytical curve built with CB and 3-MPTMS/CB. Very satisfactory figures of merit including limit of detection (LOD) of 1.33 $\mu\text{g L}^{-1}$, limit of quantification (LOQ) of 4.45 $\mu\text{g L}^{-1}$, preconcentration factor of 28.0, consumptive index of 0.714 mL, preconcentration efficiency of 5.6 min^{-1} and sample throughput of 12 h^{-1} were obtained. The precision of the method was assessed as relative standard deviation (RSD) (%) for 10 measures of 10.0 and 160.0 $\mu\text{g L}^{-1}$ Pb(II) solutions yielding values of 3.0 and 2.3 %, respectively. The preconcentration method was successfully applied to the Pb(II) ions determination in different kinds of water and *Ginkgo Biloba* samples with satisfactory recovery values (91 – 108 %). In addition, accuracy of proposed method was also checked by analysis of certified marine sediment reference material (MESS-3).

keywords: Adsorbent , carbonaceous material, silanization, on-line preconcentration, lead.

Introduction

In the last years, the search for alternative nanomaterials with large surface area, low-cost, high reusability, selectivity and chemical stability for the removal/preconcentration of pollutant metals from different sample media have been the main challenge and goal for the analytical chemists.¹ In this context, nano-carbon blacks (CB) have increasingly gained interest as alternative nanoadsorbents for the adsorption of some analytes in detriment of carbon nanotubes and activated carbon. This material is composed essentially of spherical carbon primary particles, which forms aggregates of 10 or more spheres, resulting in a large cluster of carbon layers with a pronounced ordering.²⁻⁴ In general, according to different production processes, the CB obtained presents different diameter range, as well as differently charged surface. Furnace black produces particles with diameter range from 20 nm to 80 nm and it is considered the most important production process, giving rise to materials with surface neutral or negatively charged, a particularly important characteristic for adsorption of metal ions.⁵ On the other hand, the process known as channel and thermal black produces structure of CB with particle size in the range of 9 – 30 nm and 120 – 150 nm and acidic and inactive surfaces, respectively, and their applications are limited due to their surface properties.

Approximately 90% of the world demand for CB has been used as rubber automotive products and non-automotive rubber products including industrial molded and extruded products. The remaining 10% is divided among other applications such as, pigment, UV absorbing and/or conducting agent in inks, coatings and plastics.^{4,6-9} As previously mentioned, the fine particles of CB tend to form large agglomerates due to Van der Waals forces, which in turn decreases their dispersion in polar solvent, promotes instability of dispersion and, as consequence, may decrease their applicability as adsorbent of metallic ions and synthesis of nanocomposites materials for different applications. Additionally, the

1 virgin CB depending upon the production process may contain low amount of functional
2 groups under their surface such as OH (hydroxyl), carbonyl (C=O) and COOH (carboxyl),
3
4
5 which leads to low adsorption capacity of material towards the metallic ions. In order to
6
7
8 overcome these undesirable effects and to improve the dispersability, chemical stability
9
10 and heavy metals removal efficiency, many effective approaches such as oxidation,¹⁰
11
12 surfactant adsorption,¹¹ polymer grafting¹²⁻¹⁵ and dispersant addition¹⁶ have been
13
14 proposed. The oxidation process has been the simplest approach for CB modification,
15
16 since it removes the impurities from CB structure and improves the reactivity of material
17
18 due to increase of functional groups such as carboxyl, phenolic hydroxyl and quinonic
19
20 structures.^{4,17} The removal from aqueous medium of As(VI) using CB oxidized with H₂SO₄
21
22 and Cd(II) and Cu(II) from wastewater using CB oxidized with HNO₃ has recently been
23
24 reported.^{5,18} The results obtained clearly demonstrated significant improvements on the
25
26 metal ion adsorption after chemical treatment of CB. In spite of the most of these materials
27
28 to present good adsorption of metal ions, their selectivity is limited due to presence of
29
30 oxygen atoms, which are able to uptake several metal ions (alkaline earth elements, and
31
32 transition metal).
33
34
35
36

37 The adsorption capacity of CB towards the metal ions may also be achieved through
38
39 chemical modification using organosilanes. In the surface silanization technique,
40
41 organosilanes used as surface modifiers may contain different functional groups such as
42
43 thiol, amino and pyridine, which are self-assembled on the material surface and capable to
44
45 interact with metal ions. These functional groups depending upon pH chosen may provide
46
47 better selectivity towards the transition metal ions based on the Person's theory.¹⁹ Even
48
49 though very interesting, this approach for improving the adsorption properties of CB
50
51 towards the metal ions has not been yet demonstrated. On the other hand, considerable
52
53 progresses have been achieved on the application of silanization of carbon nanotubes with
54
55 focus on metal ion preconcentration. Carbon nanotubes modified with 3-
56
57 aminopropyltriethoxysilane (AAPTS), pyridine-functionalizing agent (N-(3-
58
59
60

(triethoxysilyl)propyl)isonicotinamide, 3-mercaptopropyltrimethoxysilane (3-MPTS) have been applied to adsorption of Cr(VI), As(V) and Se(VI)²⁰, Pb(II)²¹, and Cd(II) and Pb(II).^{19,22}

Accordingly, in this paper a CB chemically modified with 3-MPTS was prepared and evaluated as adsorbent of Pb(II) aiming at development of a highly sensitive FIA-FAAS method. The material was characterized by Fourier transform infrared spectra (FT-IR), scanning electron microscopy (SEM), energy dispersive (EDS), Raman spectroscopy, as well as by thermogravimetric analysis and textural data. The choice of 3-MPTMS was based on the presence of thiol and sulfur, which have high retention capacity either of soft metals or borderline metals, as classified lead ions. The developed method was successfully applied in different types of water samples and medicinal herb (*Ginkgo Biloba*) and the accuracy of method was checked by analysis of certified reference material.

Materials and Methods

Reagents and Instruments

All solutions were prepared from analytical grade reagents and ultrapure water (resistivity $\geq 18.2 \text{ M}\Omega \text{ cm}^{-1}$) from a Millipore Milli-Q purification system (Bedford, MA, USA). To avoid any risk of contamination, all glassware were kept overnight in a 10% (v/v) HNO_3 solution and then washed with deionized water. Pb(II) working solutions were prepared from a 1000 mg L^{-1} Pb(II) standard solution purchased from Merck (Darmstadt, Germany) by making appropriate dilutions with ultrapure water. Sodium citrate and acetate buffer solutions were prepared from the respective salts without any purification (all from Merck) whereas Tris(hydroxymethyl)aminomethane hydrochloride (Tris-HCl) was obtained from Sigma-Aldrich (Steinheim, Germany). In addition, the pH of these solutions were adjusted to the desired value with NaOH (Merck) and/or HNO_3 (Vetec, Rio de Janeiro) solutions. Solutions of Fe(III), Cu(II), Ni(II), Ca(II), Mg(II), Ba(II), As(III), Cd(II) and Zn(II), used in the foreign cations studies, were prepared from their stock solutions (1000 mg L^{-1}) or from

1
2 their salts (all of analytical grade and acquired from Merck). 30% (v/v) H₂O₂ and 65% (v/v)
3
4 HNO₃, acquired from Sigma-Aldrich, were used in the microwave-assisted acid digestion
5
6 procedure. A commercial nanoscale Carbon Black (CB) with particle size of 20-70 nm was
7
8 kindly supplied by Cabot VULCAN[®] (Brasil Indústria e Comércio LTDA), whereas the
9
10 modifier reagent 3-mercaptopropyltrimethoxysilane (3-MPTMS) and ethanol, used in the
11
12 chemical modification were acquired from Sigma-Aldrich.
13
14

15 Measurements of Pb(II) were carried out in an AA-7000 flame atomic absorption
16
17 spectrophotometer (FAAS) (Shimadzu, Kyoto, Japan) equipped with a hollow cathode
18
19 lamp as radiation source (Hananatsu Photonics, K.K) and deuterium lamp as background
20
21 correction. The hollow cathode lamp was operated at 8.0 mA and the wavelength was set
22
23 at 217 nm, while the flame composition was maintained at acetylene at a flow rate of 1.5 L
24
25 min⁻¹ and air at flow rate of 10.0 L min⁻¹. A flow injection system was constructed from an
26
27 Ismatec IPC-08 peristaltic pump (Glattzbrugg, Switzerland) and Tygon[®] tubing used for
28
29 propelling samples and reagents. A homemade mini-column, made of polyethylene (3.0
30
31 cm in length and 0.70 cm at the top internal diameter) packed with 100 mg of CB modified
32
33 with 3-mercaptopropyltrimethoxysilane (3-MPTMS/CB) was coupled in a homemade
34
35 injector commutator for preconcentration and elution procedure. A small piece of cotton
36
37 tissue was fixed at the mini-column extremities by inserting the upper end of a conical tip
38
39 into the mini-column cylindrical edge, to avoid loss of material. The sample pH was
40
41 measured with a Metrohn 826 mobile digital pH meter (Herisau, Switzerland). For
42
43 characterization of the following materials: virgin nano-carbon black and modified nano-
44
45 carbon black, a Shimadzu FT-IR-8300 Fourier transform spectrometer in transmission
46
47 mode (4000 – 400 cm⁻¹) was used, whereas the surface morphology of the adsorbent
48
49 material was evaluated by a scanning electron microscopy (SEM) using a Philips FEI
50
51 Quanta 200 (Amsterdam, The Netherlands) equipped with probe of energy dispersive
52
53 spectroscopy (EDS). The thermal stability of the studied materials was analyzed on a
54
55 Perkin Elmer TGA 4000 thermogravimetric instrument in the temperature range of 30 –
56
57
58
59
60

1 800 °C (scanning rate 10 °C min⁻¹, nitrogen flow rate of 20 mL min⁻¹). Textural properties,
2 such as specific areas, average pore sizes and volumes of the virgin and modified nano-
3 carbon blacks were determined by a Quantachrome Nova 1200e automatic instrument.
4 Average pore sizes and volumes of these materials were estimated by the Barrett-Joyner-
5 Halenda (BJH) method based on nitrogen sorption experiments, whereas the specific
6 surface areas were determined from sorption isotherms according to the Brunauer-
7 Emmett-Teller (BET) method. Raman spectra were measured using a DeltaNu Advantage
8 laser Raman spectroscopy system in the range 200 – 3400 cm⁻¹. For this analysis, the
9 wavelength of the excitation beam was fixed at 532 nm and the exposure time of 15
10 seconds was adopted to prevent damage caused by laser irradiation. Certified reference
11 material (MESS-3) was decomposed in a microwave oven Milestone Ethos One (São
12 Paulo, Brazil).
13
14
15
16
17
18
19
20
21
22
23
24
25
26
27
28
29
30

31 **Functionalization of nano-carbon black by using 3-MPTMS**

32
33
34 Initially, 2.0 g of virgin nano-carbon black were oxidized with 50.0 mL of 65% HNO₃
35 under reflux at 120 °C during two hours to remove impurities from the material and
36 increase the amount of functional groups in the surface able to react with organosilane
37 modifier. The obtained material – (CB-oxi, oxidized nano-carbon black) was washed with
38 ultrapure water until reaching pH ≈ 7.0 and further dried at 100 °C. After that, 1.5 g of CB-
39 oxi were dispersed in 200.0 mL of ethanol and kept in an ultrasonic bath for 30 min. In
40 sequence, 3.0 mL of 3-MPTMS were added in this mixture and kept under reflux at 65 °C
41 for 3 hours. The obtained material was dried at 50 °C for 12 hours.^{19,23,24} The schematic
42 representation of CB functionalized with 3-MPTMS and interaction with Pb(II) are shown in
43 Figure 1.
44
45
46
47
48
49
50
51
52
53
54
55
56
57
58
59
60

On-line preconcentration procedure and optimization strategy

The on-line preconcentration system was performed loading aliquots of 20.0 mL of sample or Pb(II) standard solution, buffered (pH 4.76) with 0.0358 mol L⁻¹ acetate, through a mini-column filled with 100 mg of 3-MPTMS/CB at a flow rate of 4.0 mL min⁻¹. After the preconcentration step, the Pb(II) ions retained in the active sites of adsorbent were eluted with 2.0 HNO₃ mol L⁻¹ through the mini-column toward the FAAS detector. All absorbance signals were taken as peak height.

In order to find the best performance of the on-line preconcentration of Pb(II) ions, a 2⁵⁻¹ fractional factorial design was employed. Thus, the factors such as pH, buffer concentration (BC), eluent concentration (EC), preconcentration flow rate (PFR) and adsorbent mass (AM) which plays an important role in the preconcentration system, were evaluated and the maximum (+) and minimum (-) levels studied are shown in Table 1. After these studies, the factors sample pH and buffer concentration were studied using a Doehlert matrix for two levels. All experiments were randomly chosen, in duplicate, to avoid possible systematic errors. The significance of each factor was evaluated from the analysis of variance (ANOVA) performed at 95% confidence interval and graphically represented by a Pareto chart.

Effect of foreign ions on the Pb(II) preconcentration method

The selectivity of the proposed method for preconcentration of Pb(II) ions was evaluated through the analysis of binary solutions of the following cations: Fe(II), Cu(II), Ni(II), Ca(II), Mg(II), Ba(II), As(III), Cd(II) and Zn(II), at different proportions of the mixture analyte:interferent (w/w). The concentrations of foreign ions were chosen taking into account the maximum permissible levels in freshwater established by the Brazilian government regulating agencies.^{25,26} All experiments were performed under optimized

1 conditions and a relative error of less than 10% was considered within the experimental
2 error.
3
4
5
6
7

8 **Breakthrough curves for the adsorption of Pb(II) onto 3-MPTMS/CB at different flow rates**

9
10
11 Three breakthrough curves, at different flow rates, were constructed under dynamic
12 and optimized conditions by percolating aliquots of 1.0 and 10.0 mL of 3.0 mg L⁻¹ Pb(II)
13 solution through mini-column packed with 100 mg of 3-MPTMS/CB, until saturation was
14 reached. Each aliquot of the effluent from the mini-column was collected and analyzed by
15 FAAS. The amount of Pb(II), adsorbed on the 3-MPTMS/CB in the flow rate of 2.0, 4.0 and
16 6.0 mL min⁻¹, was determined using the equation 1 depicted below and a graph of C_f/C_i vs.
17 effluent volume (mL) plot was built, where C_f and C_i are the final and initial Pb(II)
18 concentration (mg L⁻¹), V is the solution volume (mL) and m (g) is the mass of 3-
19 MPTMS/CB.
20
21
22
23
24
25
26
27
28
29
30
31
32
33

$$34 \quad Q(\text{mg / g}) = \frac{(C_i - C_f) \cdot V}{m} \quad (\text{Equation 1})$$

35
36
37
38
39

40 **Sample preparation**

41
42 Different kinds of water samples, as well as, medicinal herb sample (Ginkgo Biloba)
43 were used to check the applicability of the proposed method. Tap water was collected in
44 the laboratory of the State University of Londrina (Londrina, Brazil) whereas the mineral
45 water and serum physiologic were acquired at a local supermarket and drugstore. Lake
46 water was collected from Igapó Lake in the city of Londrina, acidified until pH 2.0 and then
47 was filtered through a 0.45 µm cellulose acetate membrane before use. All samples were
48 spiked at 8.0 µg L⁻¹ Pb(II) concentration and its determination was performed under
49 optimum conditions using an external calibration curve. All samples studied had the pH
50
51
52
53
54
55
56
57
58
59
60

1 adjusted to 4.76 with 0.0358 mol L⁻¹ of acetate buffer solution. To check the accuracy of
2 the preconcentration method described herein, a mass of 237 mg of MESS-3 (certified
3 marine sediment reference material) was weighed into Teflon flasks and decomposed with
4 10.0 mL of the mixture concentrate HNO₃:HCl (3:1, v/v) and 1.0 mL of concentrate HF.
5
6 The mixture was kept overnight and subsequently submitted to microwave-assisted acid
7 digestion procedure under temperature program as previously reported by research
8 group.²⁷ After the sample decomposition, the solutions were heated on a hot plate almost
9 to dryness. The residues previously cooled at room temperature were dissolved in
10 ultrapure water and transferred to volumetric flasks of 100 mL. In addition, analytical
11 blanks were used to confirm the absence of interfering in the analytical system. Similarly,
12 the proposed method was applied in Ginkgo Biloba samples, weighing 500 mg and then
13 subjected to digestion process, using 10.0 mL of 65% HNO₃ and 4.0 mL of 30% H₂O₂ for
14 acid decomposition.
15
16
17
18
19
20
21
22
23
24
25
26
27
28
29
30
31
32

33 Results and discussion

34 Characterization of materials

35
36
37 Figure 2 shows the FT-IR spectra of virgin CB, CB-oxi and 3-MPTMS/CB. As can
38 be seen, intense bands observed at 3400 cm⁻¹ corresponds to the vibrations of OH group
39 from adsorbed water molecule, whereas the two bands observed at 2922 and 2850 cm⁻¹,
40 present in the 3-MPTMS/CB can be attributed to the symmetric and asymmetric stretching
41 vibrations of CH₂ and CH₃ from 3-MPTMS modifier.¹⁹ The intense band observed at 1723
42 and 1732 cm⁻¹ can be assigned to the stretching of C=O from carbonyl and/or carboxyl
43 groups present in both CB-oxi and 3-MPTMS/CB,^{4,24} while the lower band intensity at 1237
44 cm⁻¹ observed at 3-MPTMS/CB, 1234 cm⁻¹ at CB-oxi and 1113 cm⁻¹ at virgin CB, can be
45 attributed to C-O stretching vibrations.²⁸ A slight band observed at 691 cm⁻¹ can be
46 attributed Si-O vibrations, whereas the broad band at 1064 cm⁻¹ can be assigned to the Si-
47 O-C stretching vibrations from the 3-MPTMS, thus indicating the immobilization of
48
49
50
51
52
53
54
55
56
57
58
59
60

organosilane on the CB.^{19,29} The band observed at 1385 cm^{-1} for the spectrum of virgin CB, can be assigned to the O-H deformations from COOH groups, since the modification by HNO_3 favors the presence of COOH as functional groups on the surface CB.¹⁸ In addition, the presence of peaks at 1573 cm^{-1} and 1580 cm^{-1} , observed on the spectra of 3-MPTMS/CB and CB-oxi, can be related to the physically adsorbed water in the materials.³⁰

As seen in Figure 3, the morphology of materials (virgin CB, CB-oxi and 3-MPTMS/CB), as expected, showed spherical particles in shape with size, in general, lower than 200 nm, roughness surface and are considered mesoporous (average pore diameter between 2 and 50 nm).³¹ It was noticed an increase on the particles aggregation of CB after the oxidation and silanization procedures. This behavior can be attributed to the incorporation of the functional groups, such as hydroxyl, carbonyl and carboxyl (CB-oxi) and organosilane both on the surface and in the inner pores of the CB matrix, leading to a significant decrease of the specific surface areas and, as consequence, decreases the volume pore, as can be seen in Table 2.³² One should note that the average pore diameter of the CB-oxi has been lower than one achieved for the virgin CB, most likely due to the presence of hydrophilic groups on the surface of the CB-oxi, resulting in strong interaction between particles through hydrogen bonds. On the other hand, the grafting process of 3-MPTMS, a larger molecule, in the narrow pores of CB-oxi promoted a significant increase on the average pore diameter (18.65 nm).

The porosity of materials has also been evaluated by means of nitrogen adsorption isotherms (Figures 4a, 4b and 4c). As can be seen in Figure 4a, the amount of nitrogen adsorbed is small even at high relative pressure ($P/P_0 = 0.7$), thus suggesting the presence of pores of short volume and large diameter on the 3-MPTMS/CB. This type of isotherm belongs to type IV, which indicates the presence of mesopores, generating a hysteresis of the type H3 and the presence of different pores sizes presenting parallel shapes of wedge, cones and/or plates.³³ The volume of N_2 adsorbed by CB-oxi (Figure 4b) was considerably larger than one observed for 3-MPTMS/CB, even at low relative

1 pressures. Furthermore, it has been observed an almost linear behavior for the adsorption
2 and desorption isotherms for the CB-oxi material, with isotherm characteristic of type IV
3 and H2 hysteresis, with cylindrical pores and strangulations. The hysteresis observed even
4 at low relative pressure shows that CB-oxi presents a higher heterogeneity of pores size
5 among the materials studied. Finally, as shown in Figure 4c, the hysteresis phenomenon
6 for virgin CB was not observed, since this behavior is much more pronounced in
7 adsorbents with low pore volume.^{17,33} Nevertheless, it worth emphasize that the absence
8 of hysteresis does not mean the absence of porosity of the virgin CB, once some pore
9 shapes may give rise to equal adsorption and desorption process.³³

10 The efficiency of the CB silanization has also been assessed by the energy
11 dispersive spectrum (Figure 5) and elemental mapping (Figure 6). As the electron beam
12 penetrates some nanometers in the material, the technique gives an estimative of
13 elemental composition on the surface of material and not in bulk, which is considered of
14 paramount importance in adsorption process. From achieved results, a uniform distribution
15 of S and Si were observed in the surface of the 3-MPTMS/CB, revealing a good interaction
16 of the modifier reagent (3-MPTMS) with the functional groups generated at the CB surface
17 after acid treatment, without any phase of segregation. The percentage values (wt%) for C,
18 O, Si and S on the 3-MPTMS/CB material were found to be 55.9, 29.6, 7.3, 7.2
19 respectively, confirming the presence of the modifier agent on the adsorbent material
20 matrix. Bearing in mind a silanization process, the amount of Si and S obtained can be
21 considered very satisfactory by comparing with literature data^{4,34}, thus demonstrating the
22 successful of functionalization herein adopted.

23 In this work, Raman spectroscopy was used to evaluate graphitization levels of CB
24 after the chemical functionalization (Figure 7). The first-order Raman spectra of
25 carbonaceous materials are characterized mainly by two strong peaks: the G (“Graphite”)
26 band around 1600 cm^{-1} , indicative of sp^2 -hybridized carbons and the D (“defect or
27 disorder”) band around 1350 cm^{-1} , originates from sp^3 -hybridized carbons.³⁵ In addition,
28
29
30
31
32
33
34
35
36
37
38
39
40
41
42
43
44
45
46
47
48
49
50
51
52
53
54
55
56
57
58
59
60

1 the intensity ratio $I_{(D)}/I_{(G)}$ and the full width at half maximum of these bands are spectral
2 parameters that exhibit a strong relation with the microstructure of the carbonaceous
3 materials. According to Figure 7, the $I_{(D)}/I_{(G)}$ ratio decrease from 0.904 for virgin CB to 0.799
4 for 3-MPTMS/CB and CB-oxi, indicating that both the insertion of oxidizing functional
5 groups, such as organosilane on the carbonaceous matrix, promotes a decrease in
6 disorder of the graphitic structure of nano-carbon black.
7
8
9

10 Thermal stability of materials has been evaluated through thermogravimetric analysis
11 (data not shown). A weight loss of ca 2.32, 4.7 and 24.2 % for 3-MPTMS/CB, virgin CB
12 and CB-oxi, respectively, was observed in the temperature interval of 30 – 77.5 °C, which
13 is ascribed to the removal of physically adsorbed water. The higher loss of water observed
14 to CB-oxi can be attributed to the higher amount of hydrophilic groups such as, hydroxyl,
15 carbonyl and carboxylic in the surface of this materials. Virgin CB is the most thermally
16 stable material with no significant weight loss in the evaluated temperature range (30 –
17 800 °C). For 3-MPTMS/CB two well defined peaks were observed at 360 °C and 514 °C,
18 which can be attributed, respectively, to decomposition side groups created during after
19 oxidation process still present in the material and the organosilane 3-MPTMS bonded to
20 carbonaceous matrix.^{4,36} In addition, based on thermogravimetrics analysis, the higher
21 amount of residue of about 64.9% for 3-MPTMS/CB in comparison to CB-oxi (52.0 %), can
22 be explained due to the presence of silica in the modified CB, confirming the
23 functionalization process.^{4,30,37}
24
25
26
27
28
29
30
31
32
33
34
35
36
37
38
39
40
41
42
43
44
45
46
47

48 **On-line preconcentration procedure and optimization strategy**

49

50 The optimization procedure of the on-line preconcentration method was carried out
51 by using a 2^{5-1} fractional factorial design and results were analyzed through a Pareto chart
52 with a confidence interval of 95% (Figure 8). As can be observed from Pareto chart, all
53 studied variables and the majority of the interactions were statistically significant. As
54
55
56
57
58
59
60

1 regards the pH, the negative effect (-13.47) demonstrated that adsorption of Pb(II) on the
2 surface of 3-MPTMS/CB occurs preferably in acidic medium. Considering that in
3 experimental domain (pH 4-7), the 3-MPTMS bonded on the CB is in its protonated form
4 (for instance pKa of thiol group is 10.2), the results of pH on adsorption of Pb(II) can be
5 explained based on the formation of hydroxyl species, such as $\text{Pb}(\text{OH})^+$ at higher pH
6 values, which leads to less effective interaction on the surface of adsorbent. Similarly, high
7 adsorption of Pb(II) ions was observed when the buffer concentration was used in its low
8 level (0.01 mol L^{-1}). The use of concentrated buffer solution provides a highly electrolytic
9 medium, which in turn may difficult the mass transfer of Pb(II) towards binding sites of 3-
10 MPTMS/CB. The adsorbent mass (AM) was the third most important factor on the
11 preconcentration system and the use of the mini-column containing a large amount of 3-
12 MPTMS/CB provides a positive effect, which can be attributed to the higher amount of
13 active sites available on the adsorbent material. So, 100.0 mg was chosen for further
14 studies under dynamic conditions. The eluent concentration (EC) was significant at its
15 higher studied level. So, the $2.0 \text{ mol L}^{-1} \text{ HNO}_3$ was chosen for all experiments to avoid
16 possible memory effect during several preconcentration/elution steps. A negative effect
17 was observed for the flow of preconcentration (FPR) (-4.83) when experiments were
18 performed in the experimental domain (4.0 to 6.0 mL min^{-1}), thus suggesting that higher
19 flow rates decreases the analytical signal due to slow adsorption kinetics of Pb^{2+} on the
20 material. Thus, as a compromise between sensitivity and sample throughput, 4.0 mL min^{-1}
21 was set as the best condition for further experiments. According to aforementioned results,
22 it was necessary to perform the final optimization of pH and buffer concentration and, for
23 this task, a Doehlert matrix³⁸ (Figure 9) was employed whose results are expressed in
24 Table 3. To avoid systematic errors, the assays carried out in triplicate were performed
25 randomly. The quadratic model (Equation 2) obtained from Doehlert matrix was
26 considered to be statistically significant, since lack of fit was not significant [(experimental
27
28
29
30
31
32
33
34
35
36
37
38
39
40
41
42
43
44
45
46
47
48
49
50
51
52
53
54
55
56
57
58
59
60

1
2 $F_{1,2}(2.860) < \text{tabulated } F_{1,2} (18.51)]$.³⁹ Then, the pH and buffer concentration values
3
4 defined from the quadratic model were found to be 4.76 and 0.0358 mol L⁻¹, respectively.
5
6

$$\text{Abs} = -0.0926 + 0.1691\text{pH} - 0.0241\text{pH}^2 - 5.7251\text{CT} - 22.8741\text{CT}^2 + 1.6414\text{pH} \times \text{CT}$$

(Equation 2)

Effect of interfering ions on the preconcentration system

7
8
9
10
11
12
13
14
15
16
17
18
19 The effect of various interfering ions on the Pb(II) ions preconcentration was
20 investigated. For this task, 20.0 mL of binary solution containing 200.0 µg L⁻¹ Pb(II) ions at
21 different proportions (analyte:concomitant ion) (Table 4) were submitted to the optimized
22 preconcentration procedure and the results of . As shown in Table 4, in general, high
23 analytical recoveries for Pb(II) were achieved even in the presence of possible interfering
24 ions. The explanation about the absence of interference on solid phase is not an easy
25 task, but according to Pearson's theory⁴⁰ and the high adsorption capacity, Pb(II) is prone
26 to establish higher interaction with 3-MPTMS/CB when compared to the other ions. For the
27 Ba²⁺ and Mg²⁺ ions, a positive interference was observed when studied in the proportion
28 1:100 (w/w), probably due to higher affinity these ions for oxygen atoms in the flame,
29 favoring the formation of oxides, influencing strongly the thermodynamic equilibrium
30 these ions after atomization.⁴¹ On the other hand, for Fe³⁺ ions, studied in the proportion
31 1:50 (w/w), exhibited a negative interference, probably due to formation of Fe(OH)₃.
32
33
34
35
36
37
38
39
40
41
42
43
44
45
46
47
48
49
50

Analytical performance of the proposed on-line preconcentration method

51
52 The analytical performance of the proposed on-line preconcentration method was
53 estimated for the 3-MPTMS/CB material, under the optimum conditions. A linear graph
54 was constructed from solutions of Pb(II) in the concentration range from 0.0 – 220 µg L⁻¹,
55
56
57
58
59
60

1 providing the equation $Abs = 0.0025 + 0.0011[Pb(II), \mu g L^{-1}]$ with a linear correlation
2 coefficient of 0.9997. For this equation, the limits of detection and quantification, calculated
3 according to the IUPAC definition⁴², were found to be $1.33 \mu g L^{-1}$ and $4.45 \mu g L^{-1}$,
4 respectively. The precision evaluated as repeatability for 10 measures of Pb^{2+} at $10.0 \mu g L^{-1}$
5 and $160.0 \mu g L^{-1}$ concentrations, was found to be 3.0 and 2.3 % (Relative standard
6 deviation, RSD %). Under optimized conditions, the preconcentration factor (PF),
7 determined as the ratio between the slopes calculated for the Pb(II) preconcentration using
8 the 3-MPTMS/CB adsorbent and the Pb(II) without preconcentration process (direct
9 aspiration into the FAAS detector), was found to be 28. The enhanced preconcentration
10 efficiency, promoted by functionalization of CB was confirmed by the ratio between the
11 slopes obtained from two calibration curves using 3-MPTMS/CB and CB-oxi as
12 adsorbents. An increase of about 40% on the sensibility of the method was obtained when
13 3-MPTMS/CB was used as adsorbent. This result demonstrates that even CB-oxi having
14 higher surface area, its performance to uptake Pb(II) was lower than 3-MPTMS/CB, thus
15 clearly justifying the modification of CB with functional organosilanes for metal ions uptake.
16 Other figures of merit commonly evaluated, such as concentration efficiency (CE),
17 consumptive index (CI) and sample throughput (ST) were determined for assessing the
18 efficiency of the proposed method.⁴³ The concentration efficiency (CE), which is defined as
19 the preconcentration factor obtained by adsorbent during 1 min of preconcentration step
20 was found to be $5.6 min^{-1}$, whereas the consumptive index (CI), defined as the minimum
21 volume of sample required to achieve one unit of preconcentration factor, was found to be
22 $0.714 mL$. The sample throughput (ST) was $12 h^{-1}$. The analytical performance of the
23 preconcentration method was compared with previously published method using other
24 carbonaceous materials as solid phase and FAAS as detector (Table 5). The low sample
25 consumption ($20.0 mL$), as well as the wide linear range and low limit of detection can be
26 considered the highlight of the proposed method. The chemical stability of 3-MPTMS/CB
27 can also be considered an advantage of proposed method, because more than 300
28
29
30
31
32
33
34
35
36
37
38
39
40
41
42
43
44
45
46
47
48
49
50
51
52
53
54
55
56
57
58
59
60

preconcentration/elution cycles under acidic conditions were carried out without any loss of adsorption capacity. Therefore, up to now it is not possible to accurately mention the life time of mini-column, but the number of cycles already obtained is considerably very satisfactory.

Study of the adsorption capacity of 3-MPTMS/CB under dynamic conditions (breakthrough curve)

In order to evaluate the maximum adsorption capacity of 3-MPTMS/CB under dynamic conditions towards adsorption of Pb(II), breakthrough curves were performed at different flow rates. As can be seen in Figure 10, breakthrough volumes of 8.0, 10.0 and 22.0 mL for the flow rates of 2.0, 4.0 and 6.0 mL min⁻¹ were obtained, yielding adsorption of 0.024, 0.030 and 0.066 mg g⁻¹, respectively. Yet, the respective maximum adsorption capacities of 0.96, 2.06 and 2.36 mg g⁻¹ were obtained when 98.0, 240.0 and 376.0 mL of 3.0 mg L⁻¹ Pb(II) solution at 2.0, 4.0 and 6.0 mL min⁻¹ flow rates were percolated through mini-column. The results of breakthrough volumes reflect the differences on the flow rates, i.e., the higher the flow rates the greater the breakthrough volumes, due to low contact time of solution on the mini-column. On the other hand, in spite of low contact time, the breakthrough volume for flow rate of 6.0 mL min⁻¹ has been the highest one (22.0 mL), which explain the highest adsorption of 0.066 mg g⁻¹.

It worth emphasize that the new adsorbent showed a high adsorption capacity in any flow rate when compared to carbon nanotube functionalized with 3- MPTMS (0.48 mg g⁻¹).²²

Application of the method to real samples

The feasibility of the method in real samples was evaluated by analysis of different kinds of water and food samples, followed by adding known amounts of Pb(II) to samples.

1
2
3
4
5
6
7
8
9
10
11
12
13
14
15
16
17
18
19
20
21
22
23
24
25
26
27
28
29
30
31
32
33
34
35
36
37
38
39
40
41
42
43
44
45
46
47
48
49
50
51
52
53
54
55
56
57
58
59
60

The results of the method application are listed in Table 6. The percentage of recoveries by preconcentration system ranged from 90.81 to 107.63 %, which demonstrated that Pb(II) could be determined in water and food samples subjected to acid digestion without matrix effect. Furthermore, the accuracy of the method was checked from the analysis of the certified reference material MESS-3 (marine sediment). The obtained result by the method ($19.91 \pm 1.00 \text{ mg Kg}^{-1}$) was statistically equal to the Pb(II) concentration in the certified material ($21.1 \pm 0.70 \text{ mg kg}^{-1}$) at 95% confidence interval (*Student t-test*) ($n=3$) (Table 6).

Conclusion

In this paper we described the development of a new solid phase extraction method based on on-line preconcentration of Pb(II) using CB modified with 3-mercaptopropyltrimetoxysilane. The modification of CB was successfully confirmed through FT-IR, SEM, EDS, TG, Raman spectroscopy and surface analysis by the BET method. The use of 3-MPTMS/CB as a low-cost and efficient adsorbent material in detriment to other nanocarbonaceous material, such as carbon nanotubes, was assured by good analytical performance including low sample consumption, low limit of detection and applicability to a wide range of samples without any matrix effect. In summary, due to advantages of developed method assured by performance of 3-MPTMS/CB as adsorbent, the strategy herein adopted, which is still largely unexplored, may provide new insight into application on cheap and abundant nanocarbonaceous materials in the field of separation science.

Acknowledgements

The authors would like to thank the Conselho Nacional de Desenvolvimento Científico e Tecnológico (CNPq) (Project No 481669/2013-2, 305552/2013-9, 472670/2012-3), Coordenação de Aperfeiçoamento de Pessoal de Nível Superior (CAPES) (25/2014), Fundação Araucária do Paraná (163/2014), SANEPAR and Instituto Nacional de Ciência e Tecnologia de Bioanalítica (INCT) (Project No. 573672/2008-3) for their financial support and fellowships.

References

1. T. W. B. Lo, L. Aldous and R.G. Compton, *Sensors and Actuators B*, 2012, **162**, 361.
2. C. Valenzuela-Calahorra, A. Navarrete-Guijosa, M. Stitou and E.M. Cuerda-Correa, *Applied Surface Science*, 2007, **253**, 5274.
3. Z. Jiang, J. Jin, C. Xiao and X. Li, *Colloids and Surfaces A: Physicochemical Engineering Aspects*, 2012, **395**, 105.
4. M. Atif, B. Bongiovanni, M. Giorcelli, E. Celasco and A. Tagliaferro, *Applied Surface Science*, 2013, **286**, 142.
5. D. Zhou, Y. Wang, H. Wang, S. Wang and J. Cheng, *Journal of Hazardous Materials*, 2010, **174**, 34.
6. International Agency for Research on Cancer (IARC). (2010). IARC Monographs on the Evaluation of Carcinogenic Risks to Humans. In: Carbon Black, Titanium Dioxide, and Talc., vol. 93. International Agency for Research on Cancer (IARC): World Health Organization (WHO), Lyon, France.
7. International Carbon Black Association (ICBA). (2004). Carbon Black User's Guide: Safety, Health & Environmental Information.
8. R.J. McCunney, H.J. Muranko, C.M. Long, A.K. Hamade, P.A. Valberg and P. Morfeld, P. (2012). Carbon black. In: Bingham, E., Cohrssen, B. (Eds.), *Patty's Toxicology*, sixth ed., vol. 5. John Wiley & Sons.
9. M.J. Wang, S.A. Reznick, K. Mahmud and Y. Kutsoyky, (2003). Carbon black. In: Kirk-Othmer Encyclopedia of Chemical Technology, vol. 4. John Wiley & Sons.
10. C.A. Frysz and D.D.L. Chung, *Carbon*, 1997, **35**, 1111.

- 1
2
3
4
5
6
7
8
9
10
11
12
13
14
15
16
17
18
19
20
21
22
23
24
25
26
27
28
29
30
31
32
33
34
35
36
37
38
39
40
41
42
43
44
45
46
47
48
49
50
51
52
53
54
55
56
57
58
59
60
11. S.D. Gupta and S.S. Bhagwat, *Journal of Dispersion Science Technology*, 2005, **26**, 111.
 12. Z.Z. Su, W.H. Guo, Y.J. Liu, Q.Y. Li and C.F. Wu, *Polymer Bulletin*, 2009, **62**, 629.
 13. X. Li, W. Guo, Q. Zhou, S. Xu and C. Wu, *Polymer Bulletin*, 2007, **59**, 685.
 14. P. Mao, M.X. Zhou, Z.J. Jin, W.W. Kong, Z.B. Xu and D. Vadillo, *Journal of Material Science*, 2010, **45**, 1065.
 15. Q.Y. Li, N. Yu, X.J. Qiu and C.F. Wu, *Colloids and Surfaces A: Physicochemical Engineering Aspects*, 2008, **317**, 87.
 16. R.J. Pugh, T.T. Matsunaga and F.M. Fowkes, *Colloids and Surface*, 1983, **7**, 83.
 17. A. Radenovic and J. Malina, *Hemijaska Industrija*, 2013, **67**, 51.
 18. D. Borah, S. Satokawa, S. Kato and T. Kojima, *Journal of Colloid and Interface Science*, 2008, **319**, 53.
 19. M.Z. Corazza, B.F. Somera, M.G. Segatelli and C.R.T. Tarley, *Journal of Hazardous Material*, 2012, **243**, 326.
 20. H. Peng, N. Zhang, M. He, B. Chen and B. Hu, *Talanta*, 2015, **131**, 266.
 21. L. Torkian, M.M. Amini, T. Gorji and O. Sadeghi, *Arabian Journal of Chemistry*, DOI:10.1016/j.arabjc.2014.10.041 (2014).
 22. B.F. Somera, M.Z. Corazza, M.J.S. Yabe, M.G. Segatelli, E. Galunin and C.R.T. Tarley, *Water, Air and Soil Pollution*, 2012, **223**, 6069.
 23. C. Velasco-Santos, A.L. Martínez-Hernández, M. Lozada-Cassou, A. Alvarez-Castillo and V.M. Castaño, *Nanotechnology*, 2002, **13**, 495.
 24. J. Kathi, K. Y. Rhee and J.H. Lee, *Composites Part A: Applied Science Manufacturing*, 2009, **40**, 800.
 25. ANVISA (Brazilian Health Surveillance Agency). Consultation Paper No. 89, December 13, 2004. Available at (in Portuguese): <http://www4.anvisa.gov.br/base/visadoc/CP/CP%5B8998-1-0%5D.PDF>, accessed August 10, 2015.
 26. CONAMA (Brazilian Environmental Council). Resolution No. 357, March 17, 2005. Available at (in Portuguese): <http://www.mma.gov.br/conama/legiano.cfm?codlegitipo=3>, accessed: August 10, 2015.
 27. N.B. Wutke, K.M. Diniz, M.Z. Corazza, F.M. de Oliveira, E.S. Ribeiro, B.T. da Fonseca, M.G. Segatelli and C.R.T. Tarley, *Analytical Letters*, (2015). DOI: 10.1080/00032719.2015.1041025
 28. A. Kuznetsova, D.B. Mawhinney, V. Naumenko, J.T. Yate Jr, J. Liu and R.E. Smalley, *Chemical Physics Letters*, 2000, **321**, 292.

- 1
2 29. M. Baikousi, K. Dimos, A.B. Bourlinos, R. Zboril, I. Papadas, Y. Deligiannakis and M.A.
3 Karakassides, *Applied Surface Science*, 2012, **258**, 3703.
4
5 30. B.A. Ashu-Arraha, J.D. Glennon, K. Albert, *Journal of Chromatography A*, 2012, **1222**,
6 38.
7
8 31. F.M. De Oliveira, B.F. Somera, E.S. Ribeiro, M.G. Segatelli, M.J.S. Yabe, E. Galunin
9 and C.R.T. Tarley, *Industrial Engineering Chemistry Research* 2013, **52**, 8550.
10
11 32. S. Trostová, I. Stibor, J. Karpísková, Z. Kolska and V. Svorčík, *Material Letters*, 2013,
12 **102**, 83.
13
14 33. V.G. Teixeira, F.M.B. Coutinho and A.S. Gomes, *Química Nova*, 2001, **24**, 808.
15
16 34. E. Boyaci, A. Çagır, T. Shahwan and A.E. Eroglu, *Talanta*, 2001, **85**, 1517.
17
18 35. Y. Kameva and K. Hanamura, *Chemical Engineering Journal*, 2011, **173**, 627.
19
20 36. G. Vukovic, A. Marinkovic, M. Obradovi, V. Radmilovic, M. Colic, R. Aleksic and P.S.
21 Uskokovic, *Applied Surface Science*, 2009, **255**, 8067.
22
23 37. A.S.M. Chong, X.S. Zhao, A.T. Kustedjo and S.Z. Qiao, *Microporous and Mesoporous*
24 *Materials*, 2004, **72**, 33.
25
26 38. C.R.T. Tarley, G. Silveira, W.N.L. Dos Santos, G.D. Matos, E.G.P. Da Silva, M.A.
27 Bezerra, M. Miró and S.L.C. Ferreira, *Microchemical Journal*, 2009, **92**, 58.
28
29 39. B.B. Neto, I.S. Scarminio and R.E. Bruns, *Como fazer experimentos: aplicações na*
30 *ciência e na indústria*, Ed. Bookman, Campinas, 2010.
31
32 40. R.G. Pearson, *Journal of the American Chemical Society*, 1963, **85**, 3533.
33
34 41. C.R.T. Tarley, A.F. Barbosa, M.G. Segatelli, E.C. Figueiredo and P.O. Luccas, *Journal*
35 *of Analytical Atomic Spectrometry*, 2006, **21**, 1305.
36
37 42. G.L. Long and J.D. Winefordner, *Analytical Chemistry*, 1983, **55**, 712.
38
39 43. C.R.T. Tarley and M. A. Z. Arruda, *Analytical Letters*, 2005, **38**, 1427.
40
41 44. A.F. Barbosa, M.G. Segatelli, A.C. Pereira, A.S. Santos, L.T. Kubota and P.O. Luccas,
42 C.R.T. Tarley, *Talanta*, 2007, **71**, 1512.
43
44 45. M.R. Nabid, R. Sedghi, A. Bagheri, M. Behbahani, M. Taghizadeh, H.A. Oskooie and
45 M.M. Heravi, *Journal of Hazardous Material*, 2012, **203-204**, 93.
46
47 46. M. Tuzen, K.O. Saygi and M. Soylak, *Journal of Hazardous Material*, 2008, **152**, 632.
48
49 47. Z-J. Hu, Y. Cui, S. Liu, Y. Yuan and H-W, Gao, *Environmental Science Pollution*
50 *Research*, 2011, **19**, 1237.
51
52 48. M. Ghaedi, M. Montazerzohori, N. Rahimi and M.N. Biysreh, *Journal of Industrial*
53 *Engineering Chemistry*, 2013, **19**, 1477.
54
55
56
57
58
59
60

1
2 49. A. Duran, M. Tuzen, and M. Soylak, *Journal of Hazardous Materials*, 2009, **169**, 466.
3
4
5
6
7
8
9
10
11
12
13
14
15
16
17
18
19
20
21
22
23
24
25
26
27
28
29
30
31
32
33
34
35
36
37
38
39
40
41
42
43
44
45
46
47
48
49
50
51
52
53
54
55
56
57
58
59
60

Figure Captions

Figure 1. Schematic representation of CB functionalized with 3-MPTMS and interaction with Pb(II)

Figure 2. FT-IR spectra for virgin CB, CB-oxi and 3-MPTMS/CB.

Figure 3. SEM images of CB with magnification of 50000 (a) virgin (b) CB-oxi and (c) 3-MPTMS/CB. Conditions: accelerating voltage of 30.0 kV.

Figure 4. Nitrogen adsorption isotherms on (a) 3-MPTMS/CB, (b) CB-oxi and (c) virgin CB

Figure 5. EDS spectrum of 3-MPTMS/CB

Figure 6. Elemental mapping of Si and S of 3-MPTMS/CB.

Figure 7. Raman spectra of virgin CB, CB-oxi and 3-MPTMS/CB.

Figure 8. Pareto chart showing the principal effects and their interactions using absorbance as analytical response.

Figure 9. Surface response to the variables: pH and buffer concentration.

Figure 10. Breakthrough curves for the CB-3 MPT using 3.0 mg L⁻¹ Pb(II) solution at 2.0, 4.0 and 6.0 mL min⁻¹.

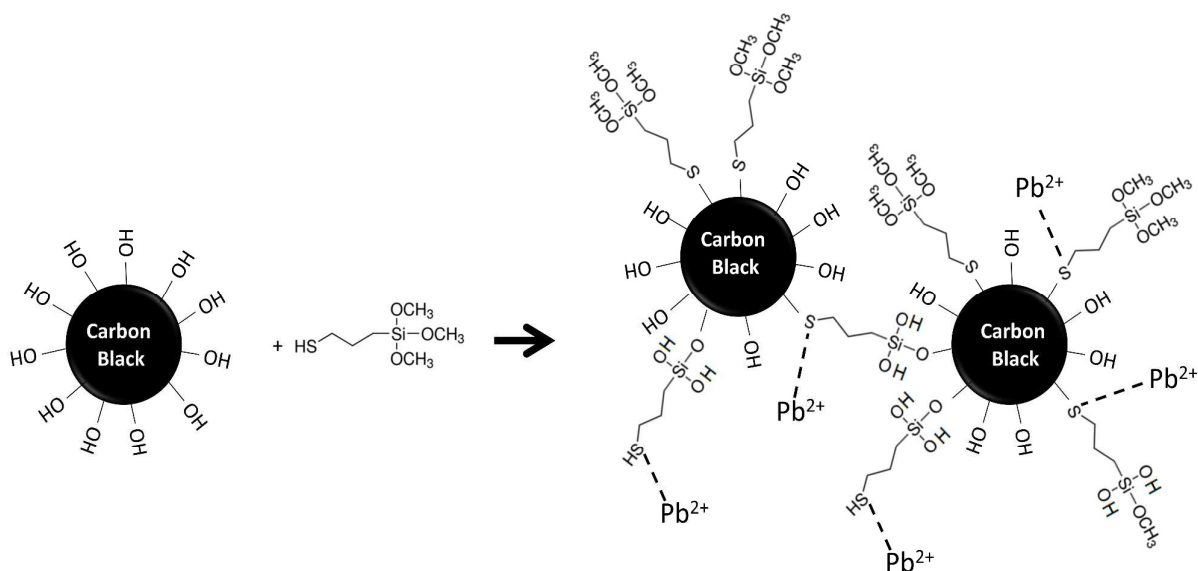


Figure 1. Nanicuacua et. al.

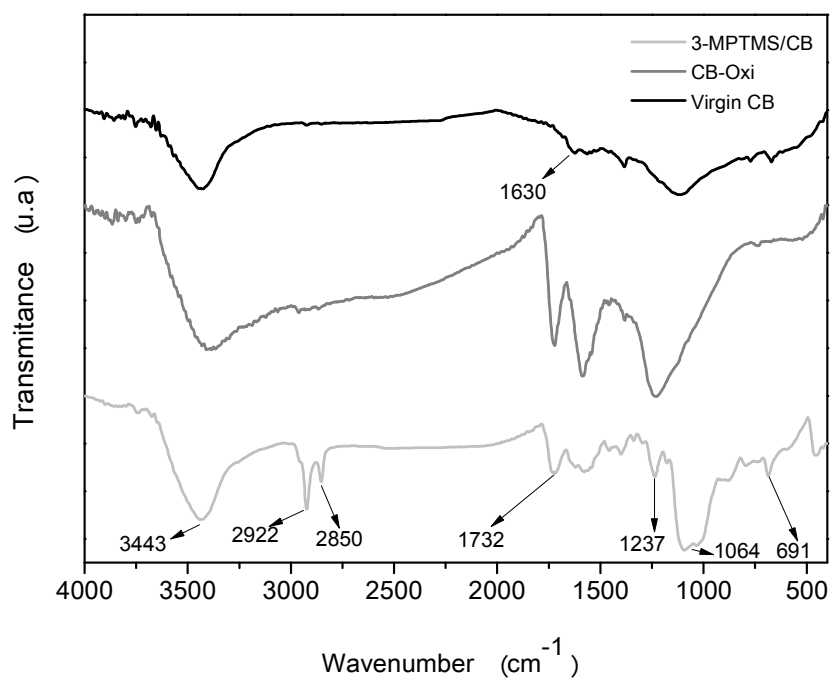


Figure 2. Nanicuacuaet. al.

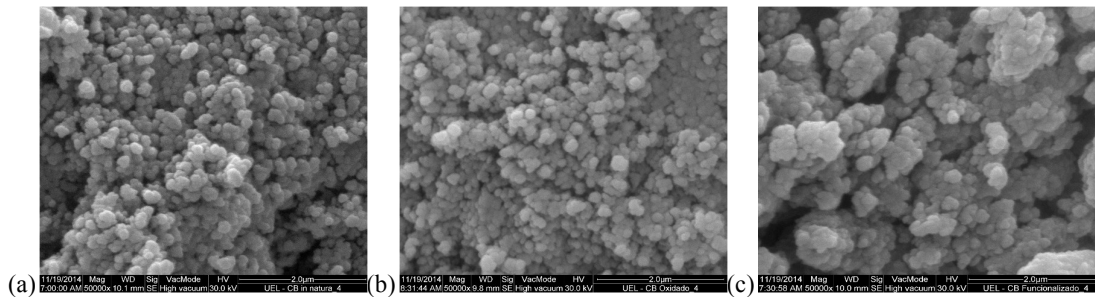
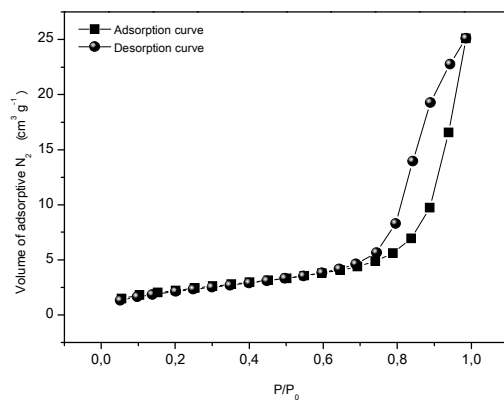
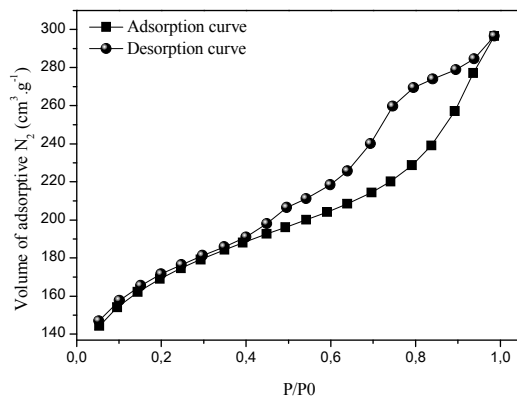


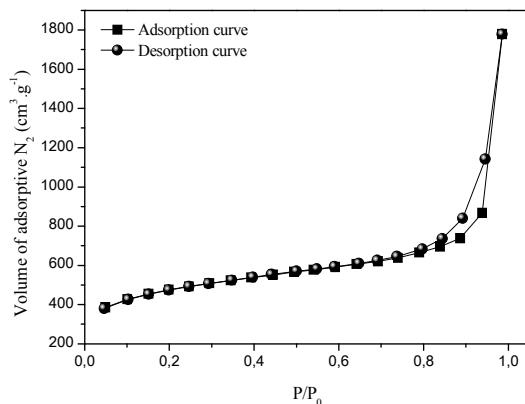
Figure 3. *Nanicuagua et. al.*



(a)



(b)



(c)

Figure 4. Nanicuacua et. al.

1
2
3
4
5
6
7
8
9
10
11
12
13
14
15
16
17
18
19
20
21
22
23
24
25
26
27
28
29
30
31
32
33
34
35
36
37
38
39
40
41
42
43
44
45
46
47
48
49
50
51
52
53
54
55
56
57
58
59
60

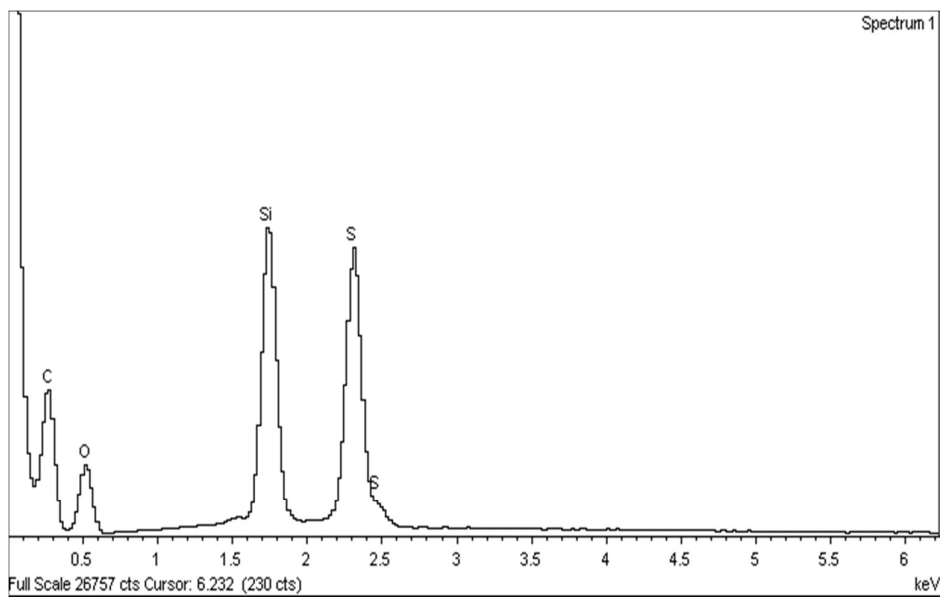


Figure 5. *Nanicuagua et. al.*

1
2
3
4
5
6
7
8
9
10
11
12
13
14
15
16
17
18
19
20
21
22
23
24
25
26
27
28
29
30
31
32
33
34
35
36
37
38
39
40
41
42
43
44
45
46
47
48
49
50
51
52
53
54
55
56
57
58
59
60

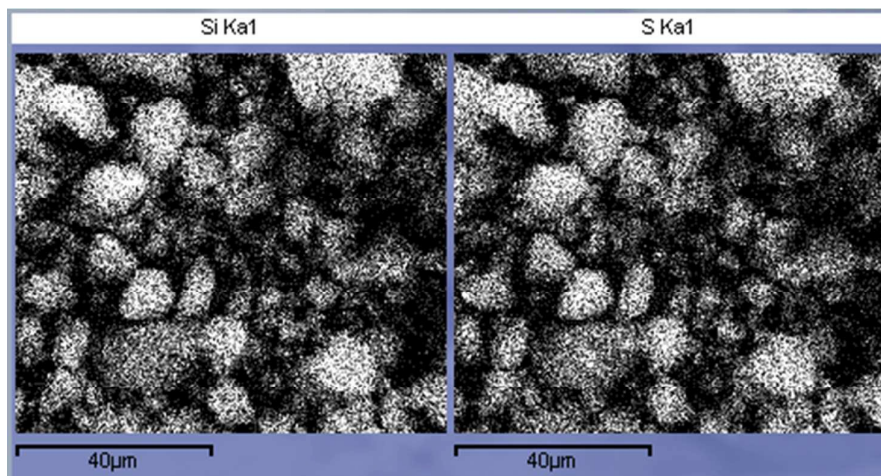


Figure 6. *Nanicuagua et. al.*

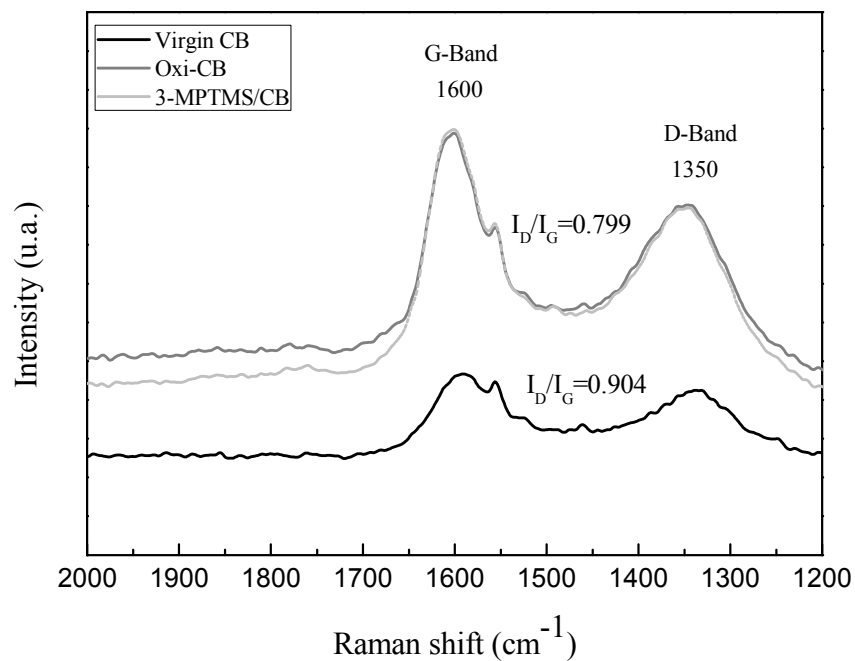


Figure 7. Nanicuacua et. al.

1
2
3
4
5
6
7
8
9
10
11
12
13
14
15
16
17
18
19
20
21
22
23
24
25
26
27
28
29
30
31
32
33
34
35
36
37
38
39
40
41
42
43
44
45
46
47
48
49
50
51
52
53
54
55
56
57
58
59
60

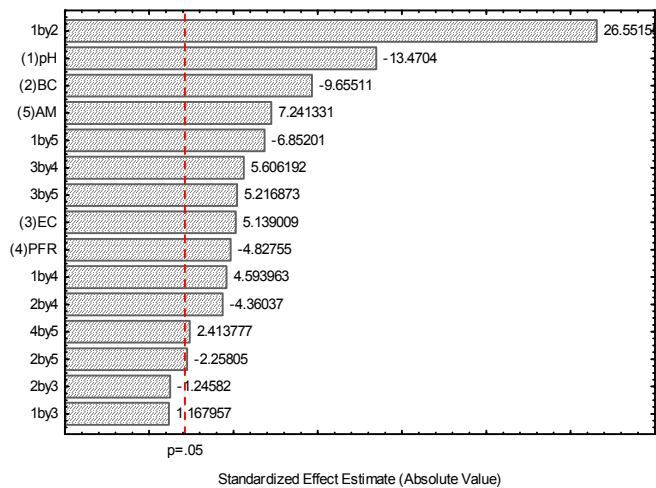


Figure 8. Nanicuacua et. al.

1
2
3
4
5
6
7
8
9
10
11
12
13
14
15
16
17
18
19
20
21
22
23
24
25
26
27
28
29
30
31
32
33
34
35
36
37
38
39
40
41
42
43
44
45
46
47
48
49
50
51
52
53
54
55
56
57
58
59
60

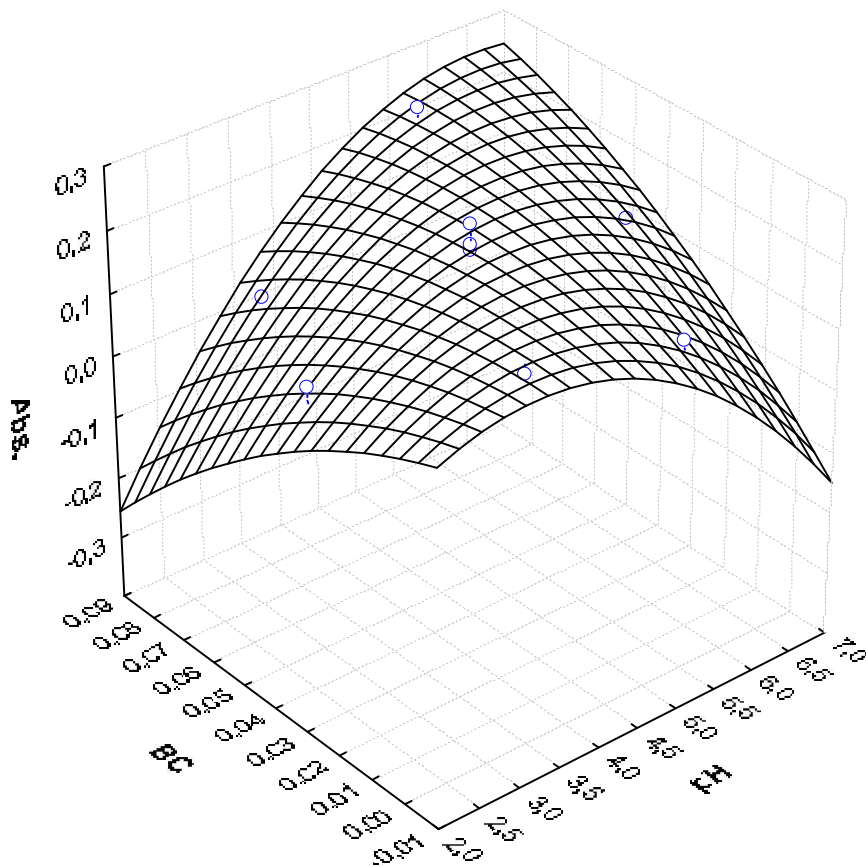


Figure 9. Nanicuacua et. al.

1
2
3
4
5
6
7
8
9
10
11
12
13
14
15
16
17
18
19
20
21
22
23
24
25
26
27
28
29
30
31
32
33
34
35
36
37
38
39
40
41
42
43
44
45
46
47
48
49
50
51
52
53
54
55
56
57
58
59
60

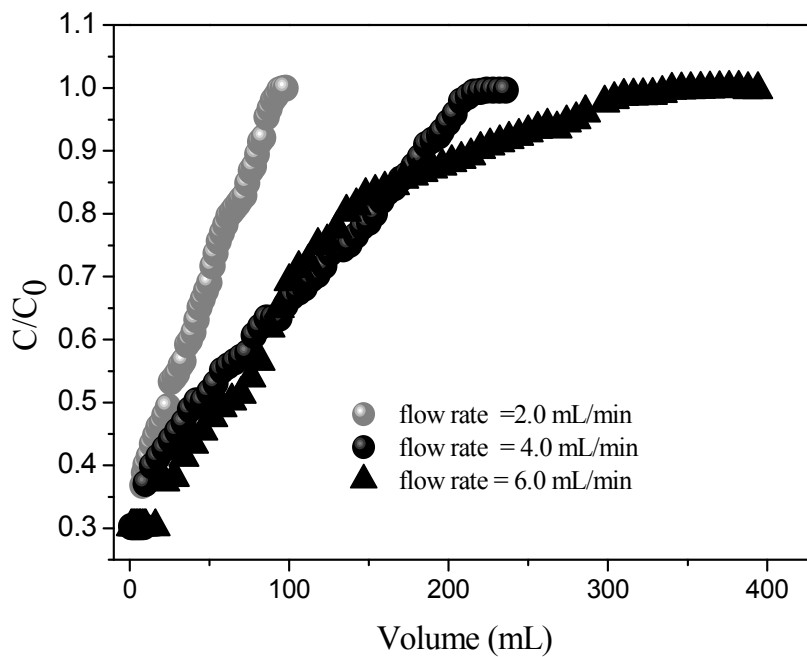


Figure 10. Nanicuacua et. al.

1
2
3
4
5
6
7
8
9
10
11
12
13
14
15
16
17
18
19
20
21
22
23
24
25
26
27
28
29
30
31
32
33
34
35
36
37
38
39
40
41
42
43
44
45
46
47
48
49
50
51
52
53
54
55
56
57
58
59
60

Table 1. Factors and their levels employed on the 2^{5-1} fractional factorial design.

| Factors | Levels | |
|--|------------------|------------------|
| | Low (-) | High (+) |
| pH | 4.0 ^a | 7.0 ^b |
| BC (mol L ⁻¹) | 0.01 | 0.1 |
| EC HNO ₃ (mol L ⁻¹) | 1.0 | 2.0 |
| PFR (mL min ⁻¹) | 4.0 | 6.0 |
| AM (mg) | 50.0 | 100.0 |

BC: buffer concentration; EC: eluent concentration; PFR preconcentration flow rate; AM: adsorbent mass. ^a = acetate/acetic acid buffer solution; ^b = Tris-HCl buffer solution

1
2
3
4
5
6
7
8
9
10
11
12
13
14
15
16
17
18
19
20
21
22
23
24
25
26
27
28
29
30
31
32
33
34
35
36
37
38
39
40
41
42
43
44
45
46
47
48
49
50
51
52
53
54
55
56
57
58
59
60

Table 2. Textural parameters of virgin CB, CB-oxi and 3-MPTMS/CB

| Carbon black | Surface area (m ² g ⁻¹) | Pore volume (cm ³ g ⁻¹) | Average pore diameter (nm) |
|--------------|---|---|----------------------------------|
| Virgin | 1573 | 2.751 | 6.99 |
| Oxidized | 551.1 | 0.458 | 3.33 |
| 3-MPTMS/CB | 8.33 | 0.039 | 18.65 |

1
2
3
4
5
6
7
8
9
10
11
12
13
14
15
16
17
18
19
20
21
22
23
24
25
26
27
28
29
30
31
32
33
34
35
36
37
38
39
40
41
42
43
44
45
46
47
48
49
50
51
52
53
54
55
56
57
58
59
60

Table 3. Doehlert matrix used on the optimization of Pb(II) solid phase preconcentration using 3-MPTMS/CB

| Assays | Buffer concentration (mol L ⁻¹) | pH | Average of absorbance (peak height) |
|--------|--|------------|--|
| 1 | 0 (0.0405) | 0 (4.5) | 0.2107 |
| 2 | 0 (0.0405) | 1 (6.5) | 0.1377 |
| 3 | 0.866 (0.081) | 0.5 (5.5) | 0.2411 |
| 4 | 0 (0.0405) | -1 (2.5) | 0.0911 |
| 5 | -0.866 (0.001) | -0.5 (3.5) | 0.1897 |
| 6 | -0.866 (0.001) | 0.5 (5.5) | 0.1273 |
| 7 | 0.866 (0.081) | -0.5 (3.5) | 0.0416 |

The first number represents the Doehlert matrix coded values, whereas the values between parentheses stand for the real values. pH 3,5, 4.5, 5.5 and 6.5 buffered with acetate/acetic acid and pH 2.5 buffered with KCl/HCl

Table 4. Effect of interfering ions on the preconcentration of Pb(II) using 3-MPTMS/CB as adsorbent

| Foreign ions | Ratio (Pb(II)/foreign ion) (w/w) | | | |
|--------------|----------------------------------|--------|--------|-------|
| | 1:1 | 1:10 | 1:50 | 1:100 |
| | % Recovery | | | |
| Zn(II) | 99.5 | 101.85 | 108.1 | 109.1 |
| Ni(II) | 103.2 | 104.4 | 104.54 | 93.0 |
| Cd(II) | 103.7 | 101.7 | 94.5 | 91.2 |
| As(III) | 107.89 | 90.78 | 100.7 | 97.3 |
| Cu(II) | 97.9 | 107.7 | 104.2 | 90.6 |
| Ca(II) | - | - | 96.2 | 107 |
| Ba(II) | - | - | 108.8 | 127.5 |
| Mg(II) | - | - | 109.8 | 127 |
| Fe(III) | 99.4 | 101.4 | 61.8 | - |

1
2
3
4
5
6
7
8
9
10
11
12
13
14
15
16
17
18
19
20
21
22
23
24
25
26
27
28
29
30
31
32
33
34
35
36
37
38
39
40
41
42
43
44
45
46
47
48
49
50
51
52
53
54
55
56
57
58
59
60

Table 5. Comparison of the analytical performance of different solid phase preconcentration for Pb(II) determination by FAAS.

| Adsorbents | Modifier | PF | Linear range ($\mu\text{g L}^{-1}$) | VP (mL) | LOD ($\mu\text{g L}^{-1}$) | Application | Ref. |
|--------------|-------------------------------------|------|--|------------|---------------------------------|---|-----------|
| MWCNT | 3-MPTMS | 31.5 | 5.0 – 130.0 | 20 | 1.71 | Waters samples and certified reference materials (PACS-2) | 22 |
| MWCNT | HNO ₃ | 44.2 | 8.6 – 775 | 20.0 | 2.6 | Waters, physiological serum, synthetic seawater, garlic and Ginkgo Biloba | 44 |
| MWCNT | Poly (2-aminothiophenol) | 304 | 3.0 – 110 | 500 | 1.00 | Water, sediment and fish samples | 45 |
| MWCNT | Ammonium pyrrolidinedithiocarbamate | 80 | --- | 400 | 0.6 | Waters samples and certified reference materials | 46 |
| MWCNT | Ethylenediamine | 60 | --- | 300 | 0.3 | Water samples | 47 |
| MWCNT | HSPIMP | 17.9 | 0.02 – 0.35 | 250 | 2.89 | Leek, radish, and banana | 48 |
| MWCNT | o-cresolphtaleincomplexone | 40 | --- | 400 | 3.52 | Real environmental water sample | 49 |
| Carbon black | 3-MPTMS | 27.5 | 10.0 – 220 | 20 | 1.36 | Waters and Ginkgo Biloba samples and certified reference material | This work |

PF = preconcentration factor; VP = volume of preconcentration; LOD = limit of detection; 3-MPTMS = 3-mercaptopropyltrimethoxysilane; HSPIMP = 3-hydroxy-4-((3-silylpropylimino)methyl) phenol.

Table 6. Application of the on-line preconcentration method of Pb(II) using CB-3 MPT as solid phase in real samples.

| Samples | [Pb ²⁺] (µg.L ⁻¹) | | Recovery (%) |
|----------------------------|---|---|--------------|
| | Amount added (µg L ⁻¹) | Amount found ^a (µg L ⁻¹) | |
| Tap water | - | ND | - |
| | 8.0 | 7.80±0.81 | 97.5 |
| Mineral water | - | ND | - |
| | 8.0 | 7.50±0.17 | 93.7 |
| Physiological serum | - | ND | - |
| | 8.0 | 8.74±0.05 | 107.6 |
| Water Igapó lake | - | ND | - |
| | 8.0 | 8.46 ± 0.03 | 105.7 |
| Ginkgo Biloba ^b | - | 0.80±0.07 | - |
| | 0.8 ^b | 1.45±0.23 | 90.8 |

ND, below limit of detection

^aResults are expressed as mean value ± standard deviation based on three replicates (n=3)^b Units expressed in µg g⁻¹

Table 7. Determination of Pb(II) in certified reference material

| | Certified value | Value founded by the analytical method ^a |
|--|-----------------|---|
| MESS-3 (marine sediment) mg Kg ⁻¹ | 21.10 ± 0.70 | 19.91 ± 1.00 |

^aResults expressed as mean ± standard deviation based on three repetitions; confidence interval of 95% (Student's t test).

1
2
3
4
5
6
7
8
9
10
11
12
13
14
15
16
17
18
19
20
21
22
23
24
25
26
27
28
29
30
31
32
33
34
35
36
37
38
39
40
41
42
43
44
45
46
47
48
49
50
51
52
53
54
55
56
57
58
59
60

1
2
3
4
5
6
7
8
9
10
11
12
13
14
15
16
17
18
19
20
21
22
23
24
25
26
27
28
29
30
31
32
33
34
35
36
37
38
39
40
41
42
43
44
45
46
47
48
49
50
51
52
53
54
55
56
57
58
59
60

GRAPHICAL ABSTRACT

